Available online at www.sciencedirect.com
SCIENCE DIRECT®
PERGAMON
Polyhedron 22 (2003) 1147–1154
POLYHEDRON
www.elsevier.com/locate/poly

Spectral and structural studies of mercury(II) complexes of 2-pyridineformamide *N*(4)-dimethylthiosemicarbazone

Elena Bermejo [a], Alfonso Castiñeiras [a,*], Isabel García [a], Douglas X. West [b]

[a] *Departamento de Química Inorgánica, Universidad de Santiago de Compostela, E-15706 Santiago de Compostela, Spain*
[b] *Department of Chemistry, University of Washington 351700, Seattle, WA 98195-1700, USA*

Received 5 December 2002; accepted 29 January 2003

Abstract

Reaction of 2-pyridineformamide *N*(4)-dimethylthiosemicarbazone (HAm4DM) with halides of mercury(II) directly afforded complexes of the form [Hg(HAm4DM)X_2] (X = Cl, Br or I). In all these new compounds, which were characterized by elemental analysis, IR spectroscopy and ^{1}H, ^{13}C, and, when possible, ^{199}Hg NMR spectroscopy, the ligand coordinates through its sulfur atom and pyridine and azomethine nitrogen atoms, as was confirmed by X-ray diffraction studies in the case of [Hg(HAm4DM)Br_2]·DMSO. Ethanolic solutions of [Hg(Am4DM)Cl_2] and [Hg(Am4DM)Br_2] afforded crystals of [Hg(Am4DM)Cl]$_2$ and [Hg(Am4DM)Br]$_2$, the structures of which were also studied by single-crystal X-ray diffractometry. In these two compounds the anionic ligand, Am4DM$^-$, coordinates to one Hg through pyridine nitrogen, imine nitrogen and thiolato sulfur atoms, the last of which bridges to the other Hg via a bond that is shorter than the chelating Hg–S bond. Thus all three of the complexes studied by X-ray diffractometry have pentacoordinated Hg centre and in all three cases the coordination polyhedron is closer to a square pyramid than to a trigonal bipyramid.

Keywords: Mercury(II) complexes; Thiosemicarbazone complexes; Crystal structures; Spectral data

1. Introduction

Thiosemicarbazones are very versatile ligands. They can coordinate to metals as neutral molecules or, after deprotonation, as anionic ligands, and can adopt a variety of different coordination modes [1]. Their antipathogenic and other biological activities in vitro depend on the N(4) substituent(s) [2]; the in vivo activity of those that are most active in vitro has been limited by their poor solubility in water [3]. We have therefore begun to explore the properties of thiosemicarbazones formed from amides, which should be relatively soluble. We have previously reported results for the following thiosemicarbazones and metal complexes thereof: 2-pyridineformamide N(4)-methylthiosemicarbazone (HAm4M) [4–6], 2-pyridineformamide thiosemicarbazone (HAm4DH) [6–8], 2-pyridineformamide N(4)-ethylthiosemicarbazone (HAm4E) [9], 2-pyridineformamide N(4)-piperidylthiosemicarbazone (HAmpip) [10–12], 2-pyridineformamide N(4)-hexamethyleniminylthiosemicarbazone (HAmhexim) [13], and 2-pyridineformamide *N*(4)-dimethylthiosemicarbazone (HAm4DM) [15]. The stoichiometry and stereochemistry of the mercury(II) complexes of this series of thiosemicarbazones have varied considerably [9]. Here, we report our results for those of HAm4DM (Fig. 1).

2. Experimental

Elemental analyses for C, H, N, and S were performed on a Carlo Erba EA model 1108 elemental analyser. Melting points were determined in open tubes with a Büchi apparatus and are uncorrected. IR spectra were obtained in the 4000–400 cm^{-1} region using KBr pellets in a Mattson Cygnus 100 spectometer, and in the 500–100 cm^{-1} region using polyethylene-sandwiched Nujol mulls in a Bruker IFS 66V spectometer. ^{1}H and

* Corresponding author. Tel.: +34-981-594-636; fax: +34-981-547-163.
E-mail address: qiac01@usc.es (A. Castiñeiras).

0277-5387/03/$ - see front matter © 2003 Elsevier Science Ltd. All rights reserved.
doi:10.1016/S0277-5387(03)00100-1

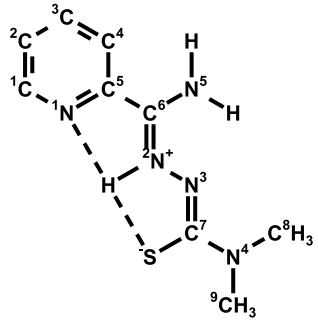

Fig. 1. Drawing of HAm4DM showing bifurcated intramolecular hydrogen bonding.

^{13}C NMR spectra were run in Bruker AMX 300 and WM 300 instruments, respectively, using DMSO-d_6 or $DCCl_3$ as solvent and TMS as internal reference. The ^{199}Hg NMR spectrum of [Hg(HAm4DM)Cl_2] was run on a Bruker AMX 500 apparatus in dimethylformamide with D_2O as solvent; the chemical shift of its single signal is expressed relative to 0.1 M $HgMe_2$. Mass spectra (FAB, 3-nitrobenzyl alcohol, Xe, 8 kV) were obtained in a Kratos MS 50 apparatus equipped with a DS-90 data acquisition system. Electron impact ionization (70 eV) was effected using the direct sample insertion system with the lowests feasible sample temperature.

All purchased chemicals were Aldrich reagent grade products, and unless otherwise specified were used as received. Solvents were purified using conventional methods. *N*(4)-dimethylthiosemicarbazide was prepared as described by Scovill [16].

2.1. Preparation of the ligand and complexes

HAm4DM was prepared as described previously [14]. The complexes were prepared as follows. A solution of HAm4DM (0.25 g, 1.12 mmol) in ethanol (20 ml) was added to a solution of the appropriate mercury(II) sal (1.12 mmol) in 20 ml of 96% ethyl alcohol, and the mixture was stirred for several days at room temperature. The resulting solids were filtered out, washed thoroughly with cold ethanol and stored in a desiccator over $CaSO_4$ until required for characterization.

2.1.1. [Hg(HAm4DM)Cl_2]

Yellow solid, (0.52 g, 93.5%): m.p. (°C) 230D. MS (FAB): $m/z = 460$ $[Hg(HAm4DM)Cl]^+$, 645 $[Hg(Am4DM)_2]^+$. *Anal.* Found: C, 21.92; H, 2.64; N, 14.74; S, 6.79%. Calc. for $C_9H_{13}Cl_2HgN_5S$ (494.79): C, 21.85; H, 2.65; N, 14.15; S, 6.48%. IR (KBr, ν/cm^{-1}): 3421m, 3341m, 3295m, 3218m (N–H); 1669s $\delta(NH_2)$; 1622m δ(NH); 1588sh (C=N); 1563s, 1526m [(C=N)+(C=C)]; 1008m (N–N); 848w (C=S); 624w (py). Far-IR (Nujol, ν/cm^{-1}): 425sh (py); 468sh, 448sh (Hg–N); 411s (Hg–S); 208s, (Hg–Cl). ^{1}H NMR (DMSO-d_6, δ/ppm): 3.27 (6H, Me); 7.71, 8.12, 8.72 (4H, py). ^{13}C NMR (DMSO-d_6, δ/ppm): 41.4 (C8, C9); 122.1 (C4); 127.0 (C2); 138.8 (C3); 144.7 (C6); 148.8 (C5); 142.3 (C1). ^{199}Hg NMR (DMF/D_2O, δ/ppm): −1059.

Single crystals of [Hg(Am4DM)Cl]$_2$ suitable for analysis by X-ray diffractometry were obtained by slow evaporation of an ethanolic solution in air at room temperature. *Anal.* Found: C, 23.73; H, 2.37; N, 15.09; S, 7.33%. Calc. for $C_9H_{12}ClHgN_5S$ (458.33): C, 23.58; H, 2.64; N, 15.28; S, 7.00%.

2.1.2. [Hg(HAm4DM)Br_2]

Yellow solid; (0.46 g, 70.0%): m.p. (°C) 294. MS (FAB): $m/z = 504$ $[Hg(HAm4DM)Br]^+$. *Anal.* Found: C, 19.37; H, 2.35; N, 12.48; S, 6.09%. Calc. for $C_9H_{13}Br_2HgN_5S$ (583.69): C, 18.52; H, 2.24; N, 12.00; S, 5.49%. IR (KBr, ν/cm^{-1}): 3397s, 3332s, 3292s, 3223s (N–H); 1659s $\delta(NH_2)$; 1618m δ(NH); 1590sh (C=N); 1552s, [(C=N)+(C=C)]; 1007m (N–N); 840m (C=S); 622w (py). Far-IR (Nujol, ν/cm^{-1}): 422w (py); 481m, 454m (Hg–N); 403m (Cd–S); 166s, 143s (Hg–Br). ^{1}H NMR (DMSO-d_6, δ/ppm): 3.26 (6H, Me); 7.69, 8.10, 8.70 (4H, py). ^{13}C NMR (DMSO-d_6, δ/ppm): 38.6 (C8, C9); 122.1 (C4); 127.1 (C2); 138.7 (C3); 144.5 (C6); 148.3 (C5); 149.5 (C1).

Single crystals of [Hg(HAm4DM)Br_2]·DMSO suitable for analysis by X-ray diffractometry were obtained by slow evaporation from a 1:1 mixture of 96% ethanol and DMSO. *Anal.* Found: C, 20.12; H, 3.00; N, 10.29; S, 9.43%. Calc. for $C_{11}H_{19}Br_2HgN_5OS_2$ (661.83): C, 19.96; H, 2.89; N, 10.58; S, 9.69%.

Single crystals of [Hg(Am4DM)Br]$_2$ suitable for analysis by X-ray diffractometry were obtained by slow evaporation of an ethanolic solution in air at room temperature. *Anal.* Found: C, 21.73; H, 2.37; N, 14.09; S, 6.33%. Calc. for $C_9H_{12}BrHgN_5S$ (502.78): C, 21.50; H, 2.41; N, 13.93; S, 6.38%.

2.1.3. [Hg(HAm4DM)I_2]

Yellow solid; (0.56 g, 73.4%): m.p. (°C) 179. MS (FAB): $m/z = 552$ $[Hg(HAm4DM)I]^+$, 647 $[Hg(HAm4DM)(Am4DM)]^+$. *Anal.* Found: C, 17.36; H, 2.07; N, 11.13; S, 5.48%. Calc. for $C_9H_{13}HgI_2N_5S$ (677.69): C, 15.95; H, 1.93; N, 10.33; S, 4.73%. IR (KBr, ν/cm^{-1}): 3431m, 3313s, 3167w (N–H); 1671s $\delta(NH_2)$; 1614sh δ(NH); 1597m (C=N); 1574m, 1525s [(C=N)+(C=C)]; 994m (N–N); 839w (C=S); 632w (py). Far-IR (Nujol, ν/cm^{-1}): 426s (py); 470s (Hg–N); 403m (Cd–S); 147s, 117m (Hg–I). ^{1}H NMR (DMSO-d_6, δ/ppm): 3.24 (6H, Me), 7.69, 8.07, 8.09, 8.69 (4H, py). ^{13}C NMR (DMSO-d_6, δ/ppm): 38.6 (C8, C9); 122.10 (C4); 126.9 (C2); 133.5 (C3); 144.6 (C6); 148.5 (C5); 148.9 (C1).

2.2. X-ray data collection, structure determination and refinement

Crystals of $[Hg(Am4DM)Cl]_2$, $[Hg(Am4DM)Br]_2$ and $[Hg(HAm4DM)Br_2]\cdot DMSO$ were mounted on glass fibers and used for data collection. Data were collected with a Nonius CAD4 diffractometer for $[Hg(Am4DM)Cl]_2$ ($\lambda = 0.71073$ Å) and for $[Hg(HAm4DM)Br_2]\cdot DMSO$ ($\lambda = 1.54184$ Å), and with a Bruker SMART CCD-1000 diffractometer for $[Hg(Am4DM)Br]_2$ ($\lambda = 0.71073$ Å). For the first two cell constants and an orientation matrix for data collection were obtained by least-squares refinement of the diffraction data from 25 reflections in the range $9.382^\circ < \theta < 12.721^\circ$ for $[Hg(Am4DM)Cl]_2$ and $15.734^\circ < \theta < 25.559^\circ$ for $[Hg(HAm4DM)Br_2]\cdot DMSO$. Data were collected at room temperature using the ω-scan technique for $[Hg(Am4DM)Cl]_2$ and $[Hg(HAm4DM)Br_2]\cdot DMSO$, and the $\omega-2\theta$ scan technique for $[Hg(Am4DM)Br]_2$. The data for $[Hg(Am4DM)Br]_2$ were processed with the programs GEMINI and SAINT [17]. The structures were solved by direct methods [18] and subsequent difference Fourier maps, which revealed the positions of all non-hydrogen atoms, and were refined on F^2 by a full-matrix least-squares procedure using anisotropic displacement parameters [19]. The N–H hydrogen atoms were located unambiguously by difference Fourier maps. The remaining hydrogen atoms were included in geometrically idealized positions employing appropriate riding models with isotropic displacement parameters constrained to 1.2 U_{eq} of their carrier atom. Atom scattering factors were taken from *International Tables for Crystallography* [20] and molecular graphics were obtained with PLATON [21]. Crystal data, experimental details and refinement results are listed in Table 1.

3. Results and discussion

The reaction of HAm4DM with HgX_2 (X = Cl, Br or I) in ethanolic solution afforded complexes with analytical data consistent with the formula $[Hg(HAm4DM)X_2]$, in which the ligand is neutral. All these complexes are stable in air and soluble in DMF and DMSO, less soluble in H_2O, MeOH, EtOH, MeCN and Me_2CO, and insoluble in $HCCl_3$ and toluene.

The mass spectra of the complexes $[Hg(HAm4DM)X_2]$ all show an ion assignable to $\{Hg(HAm4DM)X\}^+$ (at $m/z = 460$ for $[Hg(HAm4DM)Cl_2]$, 504 for $[Hg(HAm4DM)Br_2]$ and 552 for $[Hg(HAm4DM)I_2]$) and a signal at $m/z = 190$ that is probably due to $C_9H_{12}N_5$, the result of HAm4DM losing SH^- (a likely event for a structure with the bifurcated hydrogen bond shown in Fig. 1). Fragments consistent with the formation of $\{Hg(HAm4DM)(Am4DM)\}^+$ are reflected at $m/z = 645$ in the spectra of $[Hg(HAm4DM)Cl_2]$ and $[Hg(HAm4DM)I_2]$.

3.1. Spectral properties of the complexes $[Hg(HAm4DM)X_2]$

The IR spectra of the complexes $[Hg(HAm4DM)X_2]$ exhibit three bands due to the amino and imino groups in the ranges 3470–3340, 3330–3290 and 3210–3100 cm^{-1}. The imine ν(CN) band is found at 1582 cm^{-1} in the spectrum of HAm4DM [22] and at 1563, 1572 and 1574 cm^{-1} in those of $[Hg(HAm4DM)Cl_2]$, $[Hg(HAm4DM)Br_2]$ and $[Hg(HAm4DM)I_2]$, respectively, indicating coordination of the azomethine nitrogen. Consistent with this is a small shift of the ν(NN) band from 993 cm^{-1} in the spectrum of HAm4DM to 1008, 1007 and 994 cm^{-1} in those of $[Hg(HAm4DM)Cl_2]$, $[Hg(HAm4DM)Br_2]$ and $[Hg(HAm4DM)I_2]$, respectively. The expected shifts of the pyridine bands, indicating coordination of the nitrogen atom, are less evident because the 1600–1400 cm^{-1} region is complicated by the presence of thioamide bands. However, the bands due to the deformation modes appearing near 620 and 400 cm^{-1} in the spectrum of free HAm4DM are shifted to higher frequencies in those of the complexes, which is strongly indicative of HAm4DM being coordinated to the metal through the pyridine nitrogen [23]. We attribute to $\nu(HgN_{imine})$ the bands at 448, 422 and 417 cm^{-1} in the spectra of $[Hg(HAm4DM)Cl_2]$, $[Hg(HAm4DM)Br_2]$ and $[Hg(HAm4DM)I_2]$. Coordination of the thione sulfur to a soft metal centre such as Hg(II) is not expected to shift the thioamide band IV significantly; it appears at 833 cm^{-1} in the spectrum of HAm4DM, and at 845, 840 and 839 cm^{-1} in those of $[Hg(HAm4DM)Cl_2]$, $[Hg(HAm4DM)Br_2]$ and $[Hg(HAm4DM)I_2]$, suggesting some back-donation of electron density by Hg(II). The ν(HgS) bands appear in the 240–250 cm^{-1} range for all three complexes. The ν(HgCl), ν(HgBr) and ν(HgI) bands appear at 208, 166 and 147 cm^{-1}, giving ratios of 0.76 for ν(HgBr)/ν(HgCl) and 0.64 for ν(HgI)/ν(HgCl) that are in the expected ranges [24].

In the ^1H NMR spectra of the complexes the nonappearance of the N3H and N5H signals (both at 12.51 ppm in the free ligand) that in DMSO the ligand is cyclized to 2-(*N*′-dimethyl)-5-pyridine-2′-yl)-1,3,4-thiadiazole (DM134tdaz). The C1H signal (at 8.74 ppm in HAm4DM) shifts downfield in all three complexes because coordination through the pyridine nitrogen atom prevents H1 from being deshielded, as it is in the free ligand, as the result of the anisotropy of the C6=N2 bond and the proximity of the sp^2 nitrogen [25].

In the ^{13}C NMR spectra, the nonappearance of the C7 signal and deshielding of C8 in all three complexes is attributable to cyclization, coordination through the

Table 1
Crystal and structure refinement data for $[Hg(Am4DM)Cl]_2$, $[Hg(Am4DM)Br]_2$ and $[Hg(HAm4DM)Br_2]\cdot DMSO$

Compound	$[Hg(Am4DM)Cl]_2$	$[Hg(Am4DM)Br]_2$	$[Hg(HAm4DM)Br_2]\cdot DMSO$
Empirical formula	$C_{18}H_{24}Cl_2Hg_2N_{10}S_2$	$C_{18}H_{24}Br_2Hg_2N_{10}S_2$	$C_{11}H_{19}Br_2HgN_5OS_2$
Color and habit	yellow plate	yellow plate (twin)	yellow prism
Formula weight	916.67	1005.59	661.84
Crystal size (mm)	$0.40 \times 0.10 \times 0.05$	$0.25 \times 0.10 \times 0.08$	$0.25 \times 0.20 \times 0.15$
Crystal system	monoclinic	monoclinic	monoclinic
Space group	$P2_1/n$ (No. 14)	$P2_1/n$ (No. 14)	$P2_1/n$ (No. 14)
Unit cell			
a, Å	7.714(2)	7.862(2)	10.610(1)
b, Å	21.005(3)	21.234(6)	15.044(3)
c, Å	8.337(1)	8.495(3)	12.339(3)
β, °	109.31(2)	109.53(1)	102.87(2)
Volume, Å^3	1274.8(4)	1332.1(6)	1920.1(6)
Z	2	2	4
Density (Mg m^{-3})	2.388	2.507	2.289
Abs. coeff., mm^{-1}	12.432	14.696	21.355
θ Range for data collection, °	3.12–8.01	2.72–26.41	5.19–64.97
Index ranges	$-1 \leqslant h \leqslant 10$	$-9 \leqslant h \leqslant 9$	$-1 \leqslant h \leqslant 12$
	$-1 \leqslant k \leqslant 27$	$-26 \leqslant k \leqslant 26$	$0 \leqslant k \leqslant 17$
	$-11 \leqslant l \leqslant 10$	$-10 \leqslant l \leqslant 10$	$-14 \leqslant l \leqslant 14$
Max/min transmissions	0.575/0.083	0.386/0.120	0.964/0.295
Refls. collected	3905	8329	3623
Ind. refls. (R_{int})	3056(0.0267)	3035(0.0000)	3049(0.0886)
Absorption correction	ψ-scans	SADABS	ψ-scans
Data/parameters	3056/154	3025/166	3049/199
Final R indices [$I > 2\sigma(I)$]	$R_1 = 0.036$, $wR_2 = 0.0656$	$R_1 = 0.039$, $wR_2 = 0.101$	$R_1 = 0.033$, $wR_2 = 0.092$
R indices (all data)	$R_1 = 0.071$, $wR_2 = 0.072$	$R_1 = 0.039$, $wR_2 = 0.109$	$R_1 = 0.033$, $wR_2 = 0.093$
Goodness-of-fit	1.036	0.915	1.012
Largest diff. peak/hole, e Å^{-3}	1.604/−0.855	2.045/−0.646	1.032/−1.469

sulfur atom and the inductive effect of the metal. Coordination through the pyridine nitrogen atom is pointed to by the behavior of the pyridine *ortho*-carbon signals, which show deshielding of C5 and shielding of C1 [25].

^{199}Hg chemical shifts span a range of over 5000 ppm [26] and depend on the number and type of ligand atoms and the coordination geometry. In this study, only $[Hg(HAm4DM)Cl_2]$ was sufficiently soluble for ^{199}Hg NMR spectroscopy. Its spectrum exhibits a single signal at $\delta = -1059$ ppm, and the upfield shift of -8 ppm with respect to the signal of $HgCl_2$ at approximately -1051 ppm [27] is indicative of five-coordinated mercury(II) [28]. The accompanying line-broadening is attributed to chemical shift anisotropy, a common effect in ^{199}Hg NMR spectroscopy [29].

3.2. Structural properties

Of the three crystal structures only, $[Hg(HAm4DM)Br_2]\cdot DMSO$ has as its main component adduct molecular with the same stoichiometry as the first solid isolated. The two dinuclear complexes, $[Hg(Am4DM)Cl]_2$ and $[Hg(Am4DM)Br]_2$, will have arisen from the mononuclear species through partial decomposition (loss of HX) upon standing in solution. Interestingly, each of the four previously reported Hg(II) compounds prepared with 2-pyridineformamide thiosemicarbazones [9] have different stereochemistries, and that of the dinuclear complexes of this study is a fifth.

Table 2 lists selected bond lengths in the three crystals and Table 3 selected bond angles. The parameters of hydrogen bonds are listed in Table 4, and mean plane data in Table 5. Perspective views of the three adduct molecules are shown in Figs. 2–4.

Like $[Hg(HAmpip)Br_2]\cdot DMSO$ [13], $[Hg(HAm4DM)Br_2]\cdot DMSO$ is penta-coordinate, with the neutral ligand coordinating through the pyridine and azomethine nitrogen atoms and the sulfur atom. The bromo ligands bring the coordination number to five. With $\alpha = \angle(S1–Hg1–N11)$ and $\beta = \angle(N12–Hg1–Br1)$ a value of 0.23 is calculated for τ [30], indicating that the present complex is closer to a square pyramid than $[Hg(HAmpip)Br_2]$, which has $\tau = 0.27$. Thus a increases with the size of the N(4)-substituent(s), as among mercury(II) complexes with 2-acetylpyridinethiosemicarbazones [28,31].

Inspection of Table 2 shows that the bonds between Hg and the two nitrogen donors are considerably longer in $[Hg(HAm4DM)Br_2]$ than in the two dinuclear complexes, doubtless because the Hg–S bond is, as would be

Table 2
Selected bond lengths (Å) in $[Hg(Am4DM)Cl]_2$, $[Hg(Am4DM)Br]_2$ and $[Hg(HAm4DM)Br_2]\cdot DMSO$

Bond	$[Hg(Am4DM)Cl]_2$[a]	$[Hg(Am4DM)Br]_2$[b]	$[Hg(HAm4DM)Br_2]$ DMSO
Hg1–N11	2.464(5)	2.474(5)	2.554(13)
Hg1–N12	2.303(5)	2.331(6)	2.414(8)
Hg1–S1	2.694(1)	2.689(1)	2.578(3)
Hg1–S1$^{\#1}$(Br2)	2.592(2)	2.607(1)	2.589(2)
Hg1–X1	2.442(2)	2.541(1)	2.623(1)
S1–C17	1.779(6)	1.739(5)	1.665(9)
C16–N12	1.294(7)	1.284(6)	1.259(11)
N12–N13	1.371(7)	1.373(7)	1.381(12)
N13–C17	1.308(8)	1.324(7)	1.352(11)
C17–N14	1.351(8)	1.403(6)	1.340(11)
C16–N15	1.370(7)	1.369(7)	1.335(11)

Symmetry transformations used to generate equivalent atoms: [a]#1: $-x+1$, $-y$, $-z+1$; Hg1···Hg1$^{\#1}$, 3.6677(6) Å and S1···S1$^{\#1}$, 3.808(3) Å; [b]#1: $-x$, $-y$, $-z$; Hg1···Hg1$^{\#1}$, 3.6600(8) Å and S1···S1$^{\#1}$, 3.828(2) Å.

expected substantially shorter than the corresponding bonds in the latter, in which the sulfurs are bridging donors (vide infra). Both Hg–Br bonds are also longer than the Hg–Br bond of $[Hg(Am4DM)Br]_2$.

There are also significant differences in coordinating bond lengths between $[Hg(HAm4DM)Br_2]$ and $[Hg(HAmpip)Br_2]$, Hg–N11 and Hg–S being longer in the former and Hg–N12 shorter. In addition, there is a much smaller difference between the two Hg–Br distances in $[Hg(HAm4DM)Br_2]$ than between those of $[Hg(HAmpip)Br_2]$. The C16–N12 bond length in $[Hg(HAm4DM)Br_2]$, 1.259(11) Å, is the shortest in any known 2-pyridineformamide thiosemicarbazone complexes [4–15] or, indeed, any known heterocyclic thiosemicarbazone complexes [32] (cf. 1.286(5) Å in $[Hg(HAmpip)Br_2]$). The C17–S distance, 1.665(9) Å, is also shorter that the 1.689(4) Å of $[Hg(HAmpip)Br_2]$, but the other bonds of the thiosemicarbazone moiety have essentially the same lengths in these two complexes. As expected in view of the differences between their Hg-donor bond lengths, the N11–Hg–S bond angle in $[Hg(HAm4DM)Br_2]$, 128.5(3)° (Table 3), differs appreciably from the 135.42(9)° of $[Hg(HAmpip)Br_2]$ [12]. Other bond angles around Hg also differ somewhat between the two complexes, as do some of their bond angles in the thiosemicarbazone moieties.

The hydrogen bonds in $[Hg(HAm4DM)Br_2]\cdot DMSO$ are similar, though not identical, to those of $[Hg(HAmpip)Br_2]\cdot DMSO$ [11]. In both cases the strongest involve DMSO oxygen. However, whereas in

Table 3
Selected bond angles (°) in $[Hg(Am4DM)Cl]_2$, $[Hg(Am4DM)Br]_2$ and $[Hg(HAm4DM)Br_2]\cdot DMSO$

Angle	$[Hg(Am4DM)Cl]_2$[a]	$[Hg(Am4DM)Br]_2$[b]	$[Hg(HAm4DM)Br_2]$ DMSO
S1–Hg1–N12	73.61(13)	73.90(12)	72.0(2)
S1–Hg1–N11	141.96(13)	141.53(15)	128.5(3)
S1–Hg1–S1$^{\#1}$(Br2)	92.15(5)	92.58(4)	116.06(9)
S1–Hg1–X1	112.54(6)	112.99(4)	105.09(7)
N12–Hg1–N11	68.99(17)	68.32(18)	66.3(3)
N12–Hg1–S1$^{\#1}$(Br2)	105.80(13)	105.74(10)	100.0(2)
N12–Hg1–X1	136.45(13)	137.43(10)	142.19(19)
N11–Hg1–S1$^{\#1}$(Br2)	104.24(13)	104.13(14)	100.1(3)
N11–Hg1–X1	90.64(13)	90.92(12)	90.87(18)
S1$^{\#1}$(Br2)–Hg1–X1	116.61(6)	115.45(4)	113.91(5)
Hg1–S1–C17	96.4(2)	96.31(15)	102.2(3)
Hg1–N12–C16	120.9(4)	121.4(4)	121.7(7)
Hg1–N12–N13	125.2(3)	123.7(3)	119.2(5)
N15–C16–N12	122.7(6)	121.9(5)	126.7(9)
C15–C16–N12	119.0(5)	119.2(5)	119.5(9)
C16–N12–N13	113.9(5)	114.9(5)	117.2(9)
N12–N13–C17	117.8(5)	117.2(4)	118.5(8)
N13–C17–N14	116.4(5)	113.5(4)	113.8(8)
N13–C17–S1	126.3(5)	128.2(3)	123.4(7)
N14–C17–S1	117.2(5)	118.2(4)	122.8(7)

Symmetry transformations used to generate equivalent atoms: [a]#1: $-x+1$, $-y$, $-z+1$; Hg1–S1–Hg1$^{\#1}$ = 87.85(5)°; [b]#1: $-x$, $-y$, $-z$; Hg1–S1–Hg1$^{\#1}$ = 87.42(4)°.

Table 4
Hydrogen bonds (Å, °) in $[Hg(Am4DM)Cl]_2$, $[Hg(Am4DM)Br]_2$ and $[Hg(HAm4DM)Br_2]\cdot DMSO$

Compound	D	d(D–H)	d(H···A)	d(D···A)	∠(DHA)
$[Hg(Am4DM)Cl]_2$	N15–H15B···N13	0.95	2.04	2.591(7)	115.4
$[Hg(Am4DM)Br]_2$[a]	N15–H15A···Br1$^{\#2}$	0.69	3.13	3.585(5)	127.1
$[Hg(HAm4DM)Br_2]$ DMSO[b]	N13–H13···O2$^{\#1}$	0.86	2.28	2.853(10)	124.1
	N15–H15A···O2	0.86	2.13	2.906(9)	150.4
	N15–H15B···Br1$^{\#2}$	0.86	2.84	3.553(7)	142.0

Symmetry transformations used to generate equivalent atoms: [a]#1: $-x, -y, -z$; #2: $-x, -y, -z+1$; [b]#1: $-x+1, -y+1, -z$; #2: $-x, -y+1, -z$.

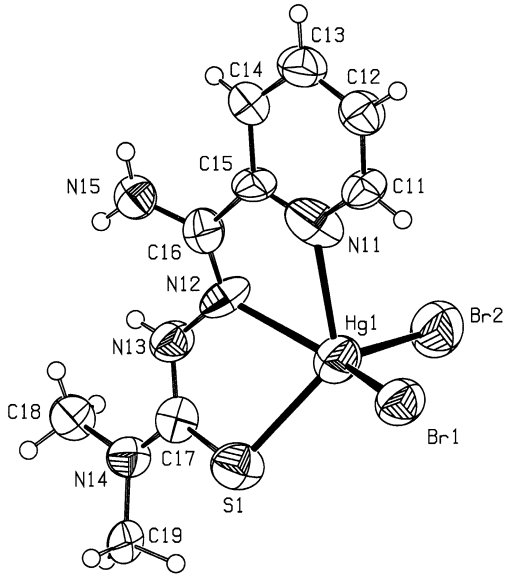

Fig. 2. Molecular structure of $[Hg(HAm4DM)Br_2]$ at 50% probability, showing the numbering scheme.

$[Hg(HAmpip)Br_2]\cdot DMSO$ N13–H and one of the N15 hydrogens both interact with the oxygen of a single DMSO molecule, in $[Hg(HAm4DM)Br_2]\cdot DMSO$ they interact with two different DMSO molecules. This difference probably results from the smaller N(4)–substituent of HAm4DM allowing more intermolecular interactions. The angle between the mean planes of the thiosemicarbazide moiety and pyridine ring in $[Hg(HAm4DM)Br_2]$, 10.19(0.44)°, is narrower than the 13.0(0.2)° found in $[Hg(HAmpip)Br_2]$, but the thiosemicarbazide moiety itself is much less planar in the former, with C16 and N12 lying at significant distances from the mean plane, doubtless because of the short C16–N12.

As noted above, the dinuclear complexes $[Hg(Am4DM)Cl]_2$ and $[Hg(Am4DM)Br]_2$ exhibit a new fifth stereochemistry for mercury(II) complexes of 2-pyridineformamide thiosemicarbazones. As in $[Hg(Am4DH)Br]_n$, where Am4DH is the anion of 2-pyridineformamide thiosemicarbazone [8], their Hg atoms are penta-coordinated, coordinating to the halo ligand, to the pyridine nitrogen, azomethine nitrogen and sulfur atoms of the tridentate anionic thiosemicarbazone, and to the sulfur of a neighboring monomer; but whereas in $[Hg(Am4DH)Br]_n$ the bridging thiolato sulfur donors link the monomers in a polynuclear chain, in the present dinuclear complexes they form centrosymmetric dimers. In the thiolato sulfur bridges the chelating Hg–S bond is longer than the other, although the difference is not as large as in $[Hg(Am4DH)Br]_n$ [8]. The τ values [30] are 0.09 for $[Hg(Am4DM)Cl]_2$ and 0.07 for $[Hg(Am4DM)Br]_2$, which are thus much closer to square pyramidal coordination geometry than $[Hg(Am4DH)Br]_n$, for which $\tau = 0.33$ [8].

With regard to their Hg-donor bond lengths the dinuclear complexes are more similar to each other than $[Hg(Am4DM)Br]_2$ is to $[Hg(Am4DH)Br]_n$ [8]. In $[Hg(Am4DM)Br]_2$ the Hg–N11 bond is shorter and the Hg–N12, Hg–S1 and Hg–S1a bonds longer than in

Table 5
Mean plane data for $[Hg(Am4DM)Cl]_2$, $[Hg(Am4DM)Br]_2$ and $[Hg(HAm4DM)Br_2]$ DMSO

Compound	Plane	Mean dev. (Å)	Largest dev. (Å)	∠ with previous plane (°)
$[Hg(Am4DM)Cl]_2$ [a]	N11–N12–S1–Cl1	0.1915	N12, 0.250(3)	–
	C16–N12–N13–C17–S1–N14	0.0220	N12, 0.039(4)	16.8(1)
	N11–C11–C12–C13–C14–C15	0.0088	C13, 0.013(5)	2.1(3)
$[Hg(Am4DM)Br]_2$ [b]	N11–N12–S1–Br1	0.1872	N12, 0.246(3)	–
	C16–N12–N13–C17–S1–N14	0.0201	N12, 0.040(3)	15.9(1)
	N11–C11–C12–C13–C14–C15	0.0143	C11, 0.023(6)	4.6(3)
$[Hg(HAm4DM)Br_2]$ DMSO	C16–N12–N13–C17–S1–N14	0.1369	N12, 0.248(7)	–
	N11–C11–C12–C13–C14–C15	0.0421	C15, 0.073(7)	10.2(4)

[a] Hg1 is 0.655(2) Å from the N11–N12–S1–Cl1 mean plane.
[b] Hg1 is 0.646(2) Å from the N11–N12–S1–Br1 mean plane.

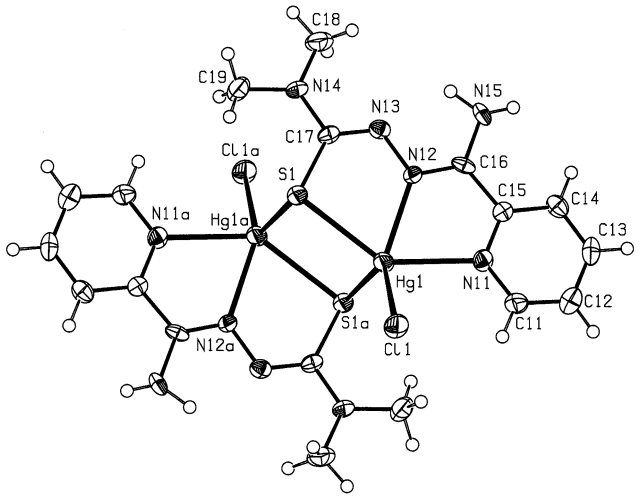

Fig. 3. Molecular structure of $[Hg(Am4DM)Cl]_2$ at 50% probability showing the numbering scheme. Symmetry transformations used to generate equivalent atoms, (a) $-x+1, -y, -z+1$.

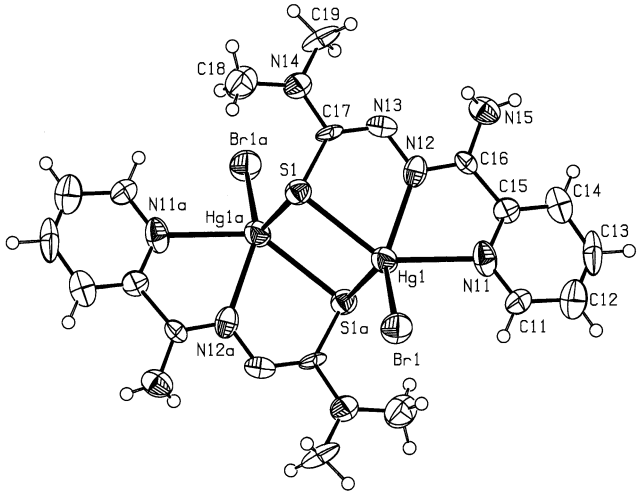

Fig. 4. Molecular structure of $[Hg(Am4DM)Br]_2$ at 50% probability showing the numbering scheme. Symmetry transformations used to generate equivalent atoms, (a) $-x, -y, -z$.

$[Hg(Am4DH)Br]_n$, and the thiosemicarbazone moiety has a longer C17–N14 bond and a shorter C17–S bond than that of $[Hg(Am4DH)Br]_n$, in which these two bonds have essentially the same lengths as in $[Hg(Am4DM)Cl]_2$. There are no major differences in bond angles between $[Hg(Am4DM)Cl]_2$ and $[Hg(Am4DM)Br]_2$, but there are between the latter and $[Hg(Am4DH)Br]_n$, especially as regard all the angles involving the bridging sulfur, for example, in $[Hg(Am4DH)Br]_n$ $\angle(S1–Hg1–S1a) = 122.38(8)^\circ$ [8], and in $[Hg(Am4DM)Br]_2$ $92.58(4)^\circ$.

$[Hg(Am4DM)Cl]_2$ has a strong intraligand N15–H15 ···N13 hydrogen bond, that is not present in $[Hg(Am4DM)Br]_2$, which instead has a weak interaction between N15–H and a bromo ligand of a neighboring molecule (Table 4). In $[Hg(Am4DH)Br]_n$, both N15 hydrogens interact strongly with bromo ligands of neighboring molecules [8]. The Am4DM ligands in $[Hg(Am4DM)Cl]_2$ and $[Hg(Am4DM)Br]_2$ are nearly planar, with just small angles between the mean planes of the pyridine ring and thiosemicarbazide moiety (Table 5). The four donor atoms defining the base of the square pyramid surrounding the Hg atom deviate considerably from coplanarity.

4. Conclusion

Complexes of stoichiometry $[Hg(HAm4DM)X_2]$ were isolated from the reactions of HAm4DM with $HgCl_2$, $HgBr_2$ and HgI_2. Crystals of $[Hg(HAm4DM)Br_2]\cdot$ DMSO and of the dinuclear, centrosymmetric complexes $[Hg(Am4DM)Cl]_2$ and $[Hg(Am4DM)Br]_2$ were obtained that were suitable for study by X-ray diffractometry. In all three of these latter compounds the mercury(II) centres are penta-coordinated. The dinuclear complexes, which both contain the anionic ligand $Am4DM^-$, are very similar in many respects, but $[Hg(Am4DM)Br]_2$ has a C–S bond that is surprisingly short for a bridging sulfur and a long C–N4 bond. The stereochemistry of these dimers is the fifth kind found among mercury(II) complexes of 2-pyridineformamide thiosemicarbazones.

5. Supplementary material

Crystallographic data (excluding structure factors) for the structures reported in this paper have been deposited with the Cambridge Crystallographic Data Center as Supplementary Publications Nos. CCDC-199 152 (for $[Hg(Am4DM)Cl]_2$), CCDC-199 153 (for $[Hg(Am4DM)Br]_2$) and CCDC-199 154 (for $[Hg(HAm4DM)Br_2]$ DMSO). Copies of this material can be obtained, free of charge, on application to the Director, CCDC, 12 Union Road, Cambridge CB21EZ, UK, (fax: +44-1223-336033 or e-mail: deposit@ccdc.cam.ac.uk).

References

[1] (a) M.J.M. Campbell, Coord. Chem. Rev. 15 (1975) 279;
(b) E.S. Raper, Coord. Chem. Rev. 61 (1985) 115;
(c) D.X. West, S.B. Padhye, P.B. Sonawane, Struct. Bonding (Berlin) 76 (1991) 4;
(d) J.S. Casas, M.S. García-Tasende, J. Sordo, Coord. Chem. Rev. 209 (2000) 49.
[2] (a) M.C. Miller, C.N. Stineman, J.R. Vance, D.X. West, I.H. Hall, Anticancer Res. 18 (1998) 4131;
(b) M.C. Miller, C.N. Stineman, J.R. Vance, D.X. West, I.H. Hall, Appl. Organomet. Chem. 13 (1999) 9;
(c) I.H. Hall, B.J. Barnes, J.E. Rowell, K.A. Shaffer, S.E. Cho, D.X. West, A.M. Stark, Pharmazie 56 (2001) 648.

[3] D.X. West, unpublished results based on reports from the National Cancer Institute, Bethesda, MD, USA.
[4] D.X. West, J.K. Swearingen, J. Valdés-Martínez, S. Hernández-Ortega, A.K. El-Sawaf, F. van Meurs, A. Castiñeiras, I. Garcia, E. Bermejo, Polyhedron 18 (1999) 2919.
[5] D.X. West, J.K. Swearingen, A.K. El-Sawaf, Transit. Met. Chem. 25 (2000) 87.
[6] I. García, E. Bermejo, A.K. El-Sawaf, A. Castiñeiras, D.X. West, Polyhedron 21 (2002) 729.
[7] A. Castiñeiras, I. Garcia, E. Bermejo, D.X. West, Z. Naturforsch. B55 (2000) 511.
[8] A. Castiñeiras, I. Garcia, E. Bermejo, D.X. West, Polyhedron 19 (2000) 1873.
[9] I. Garcia, Ph.D. Thesis, University of Santiago de Compostela, 2001.
[10] K.A. Ketcham, J.K. Swearingen, A. Castiñeiras, I. Garcia, E. Bermejo, D.X. West, Polyhedron 20 (2001) 3265.
[11] A. Castiñeiras, I. García, E. Bermejo, K.A. Ketcham, D.X. West, A.K. El-Sawaf, Z. Anorg. Allg. Chem. 628 (2002) 492.
[12] K.A. Ketcham, I. Garcia, J.K. Swearingen, A.K. El-Sawaf, E. Bermejo, A. Castiñeiras, D.X. West, Polyhedron 21 (2002) 859.
[13] K.A. Ketcham, I. Garcia, E. Bermejo, J.K. Swearingen, A. Castiñeiras, D.X. West, Z. Anorg. Allg. Chem. 628 (2002) 409.
[14] E. Bermejo, A. Castiñeiras, L.M. Fostiak, I. Garcia, A.L. Llamas, J.K. Swearingen, D.X. West, Z. Naturforsch. 56b (2001) 1297.
[15] L.M. Fostiak, I. Garcia, J.K. Swearingen, E. Bermejo, A. Castiñeiras, D.X. West, Polyhedron 22 (2003) 83.
[16] J.P. Scovill, Phosphorus, Sulfur Silicon 60 (1991) 15.
[17] SMART and SAINT. Area Detector Control and Integration Software, Bruker Analytical X-ray Instruments Inc., Madison, WI, USA, 1997.
[18] G.M. Sheldrick, Acta Crystallogr., Sect. A 46 (1990) 467.
[19] G.M. Sheldrick, SHELX-97. Program for the Refinement of Crystal Structures, University of Göttingen, Germany, 1997.
[20] A.J.C. Wilson (Ed.), International Tables for Crystallography, vol. C, Kluwer Academic Publishers, Dordrecht, The Netherlands, 1995.
[21] A.L. Spek, PLATON. A Multipurpose Crystallographic Tool, Utrecht University, Utrecht, The Netherlands, 2002.
[22] D.X. West, J.K. Swearingen, J. Valdés-martínez, S. Hernández-Ortega, F. Van Meurs, A. Castiñeiras, I. García, E. Bermejo, Polyhedron 18 (1999) 2919.
[23] D.K. Rastoh, K.C. Sharma, J. Inorg. Nucl. Chem. 36 (1974) 2219.
[24] K. Nakamoto, Infrared and Raman Spectra of Inorganic and Coordination Compounds, 2nd ed., Wiley, New York, 1986.
[25] I. Antonini, F. Claudi, P. Franchetti, M. Grifantini, S. Morelli, J. Med. Chem. 20 (1977) 447.
[26] B. Wrackmeyer, R. Contreras, Annual Reports on NMR Spectroscopy, Academic Press, San Diego, CA, 1992, p. 267.
[27] A.A. Isab, H.P. Perzanowski, J. Coord. Chem. 21 (1990) 247.
[28] E. Bermejo, R. Carballo, A. Castiñeiras, R. Domínguez, A.E. Liberta, C. Maichle-Mössmer, M.M. Salberg, D.X. West, Eur. J. Inorg. Chem. (1999) 965.
[29] L. Bresolin, R.A. Burrow, M. Hörner, E. Bermejo, A. Castiñeiras, Polyhedron 16 (1997) 3947.
[30] A.W. Addison, T.N. Rao, J. Reedijk, J. van Rijn, C.C. Verschoor, J. Chem. Soc., Dalton Trans. (1984) 1349.
[31] (a) E. Bermejo, R. Carballo, A. Castiñeiras, R. Dominguez, C. Maichle-Mössmer, J. Strähle, D.X. West, Polyhedron 18 (1999) 3695;
(b) E. Bermejo, R. Carballo, A. Castiñeiras, R. Domínquez, C. Maichle-Mössmer, A.E. Liberta, D.X. West, Z. Naturforsch. 54b (1999) 777;
(c) E. Bermejo, A. Castiñeiras, R. Domínguez, R. Carballo, C. Maichle-Mössmer, J. Strähle, D.X. West, Z. Anorg. Allg. Chem. 625 (1999) 961.
[32] J.K. Swearingen, D.X. West, Transit. Met. Chem. 26 (2001) 252 (and references therein).